

Real-structure effects: Absorption edge of $\text{Mg}_x\text{Zn}_{1-x}\text{O}$, $\text{Cd}_x\text{Zn}_{1-x}\text{O}$, and n -type ZnO from *ab-initio* calculations

André Schleife^{a,c} and Friedhelm Bechstedt^{b,c}

^aCondensed Matter and Materials Division, Lawrence Livermore National Laboratory, Livermore, California 94550, USA;

^bInstitut für Festkörpertheorie und -optik, Friedrich-Schiller-Universität, Max-Wien-Platz 1, 07743 Jena, Germany;

^cEuropean Theoretical Spectroscopy Facility (ETSF)

ABSTRACT

The continuously increasing power of modern supercomputers renders the application of more and more accurate parameter-free models to systems of increasing complexity feasible. Consequently, it becomes possible to even treat different real-structure effects such as alloying or n -doping in systems like the technologically important transparent conducting oxides. In this paper we outline how we previously used a combination of quasiparticle calculations and a cluster expansion scheme to calculate the fundamental band gap of $\text{Mg}_x\text{Zn}_{1-x}\text{O}$ and $\text{Cd}_x\text{Zn}_{1-x}\text{O}$ alloys. We discuss the results in comparison to values for In_2O_3 , SnO_2 , SnO , and SiO_2 . In addition, we discuss our extension of the Bethe-Salpeter approach that has been used to study the interplay of excitonic effects and doping in n -type ZnO. The dependence of the Burstein-Moss shift on the free-carrier concentration is analyzed.

Keywords: real-structure effects, *ab initio* electronic structure methods, fundamental band gaps, optical absorption, alloy, degenerate electron gas

1. INTRODUCTION

The transparent conducting oxides (TCOs) form a highly interesting class of materials,¹ especially because the realization of transparent electronic² components has numerous consumer electronics applications with a large economic potential. In addition, such components are also beneficial, for instance, for photovoltaic applications.^{3,4} Large fundamental band gaps are a common feature of the different TCOs and explain their transparency for visible light that even extends into the ultraviolet (UV) spectral region. Oftentimes the TCOs are found to be intrinsically n -type and, hence, conductive.

The large interest in the TCOs has led to significant efforts to understand their basic properties. Consequently, ground-state properties⁵ such as lattice constants and cohesive energies, but also the electronic structures and the optical properties^{6,7} of the bulk oxides MgO, ZnO, and CdO are well understood both theoretically and experimentally^{8,9,10} nowadays. However, in order to optimize a material for a certain application, it is typically desirable or even necessary to tune certain properties. In this context, the alloying of two or more materials has been successfully applied to tailor, for instance, the lattice parameters or the fundamental band gaps.^{11,12,13} While the intrinsic electron conductivities of the TCOs are too low for applications, the free-carrier concentrations can be significantly enhanced by means of n doping.^{14,15}

In this short review paper we outline how two *ab-initio* techniques, that belong to the realm of many-body perturbation theory, can be used and extended to take two different real-structure effects into account and, hence, prove very helpful for computer-aided materials design. In Section 2 we compare numerical results for the fundamental band gaps of $\text{Mg}_x\text{Zn}_{1-x}\text{O}$ and $\text{Cd}_x\text{Zn}_{1-x}\text{O}$ alloys, that are computed by combining quasiparticle (QP) calculations with a cluster expansion approach,¹⁶ to the band gaps of several other TCOs. In Section 3 we discuss the impact of excitonic effects and n doping on the optical absorption edge of ZnO and, in particular, we quantify the differences between results from parameter-free calculations of the Burstein-Moss shift (BMS) and values obtained using a parabolic two-band model. Section 4 summarizes the paper.

Further author information:

A. Schleife: E-mail: a.schleife@llnl.gov, Telephone: +1 925 422 4216

F. Bechstedt: E-mail: bech@iftophysik.uni-jena.de, Telephone: +49 3641 947150

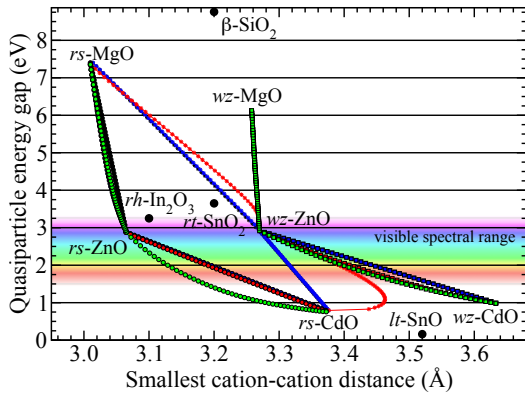


Figure 1. (Color online) Quasiparticle band gap as a function of the smallest cation-cation distance for isostructural wz (squares) and rs (small dots) as well as heterostructural (stars) $Mg_xZn_{1-x}O$ and $Cd_xZn_{1-x}O$ alloys. Configurational averages are depicted as calculated from the MDM (black), the SRS (green) as well as the GQCA for $T = 300$ K (blue) and $T = 1100$ K (red). In addition, the QP band gaps of rh - In_2O_3 , rt - SnO_2 , lt - SnO , and β - SiO_2 are indicated.

2. $Mg_xZn_{1-x}O$ AND $Cd_xZn_{1-x}O$ ALLOYS

The potential for band-gap tailoring renders pseudobinary alloys of MgO , ZnO , and CdO interesting for optoelectronic applications and devices. In experiments it has been found^{11,12,13} that the absorption onset can be shifted further into the UV spectral region, e.g., from about 3.4 eV [wurtzite- (wz) ZnO] up to ≈ 4.4 eV ($Mg_xZn_{1-x}O$). The band gap of pseudobinary $Cd_xZn_{1-x}O$ can be decreased into the visible spectral range.^{17,18} By combining recent theoretical-spectroscopy approaches with a cluster-expansion scheme, it is possible to understand the electronic and optical properties of the group-II oxide alloys as well as how different growth conditions influence these, based on *ab-initio* calculations.^{16,19,20,21} Since the equilibrium crystal structures of these oxides [wz and rocksalt (rs)] are dissimilar, their heterostructural combination is of particularly high interest.

The thermodynamic properties and the structural composition of iso- and heterostructural $Mg_xZn_{1-x}O$ and $Cd_xZn_{1-x}O$ alloys have been discussed in Ref. 19. Their electronic structure and optical properties, calculated via the HSE+ G_0W_0 scheme^{22,23,24} and the Bethe-Salpeter equation (BSE),^{25,26} respectively, are presented in Refs. 16, 20, 21. The result in Fig. 1 shows configurational averages for the difference of the QP energies of the lowest conduction-band (CB) state and the highest valence-band state obtained for thermodynamic equilibrium [based on the generalized quasi-chemical approximation^{27,28} (GQCA)] as well as non-equilibrium [using the strict-regular solution (SRS) model²⁹ and the microscopic decomposition model¹⁹ (MDM)] conditions. Significant deviations from the linear variation of the fundamental band gap with the second-nearest-neighbor distance can occur for the GQCA as well as the SRS model. The bowing of the SRS curves, i.e. their deviation from a linear behavior, is larger for the compounds in the rs crystal structures. In addition, it can be seen that there is a strong temperature dependence of the results for the heterostructural alloys. Therefore, we conclude that the preparation conditions sensitively affect these results since they have an impact on the cation distribution which influences both lattice geometries and band gaps. Comparing bowing parameters, e.g. for the composition dependence of the fundamental band gaps to experimental results and to other calculated results shows satisfactory agreement.^{16,20,21}

In this work we want to discuss configurational averages for the fundamental band gaps of the $Mg_xZn_{1-x}O$ and the $Cd_xZn_{1-x}O$ alloys and, hence, their absorption edges with respect to the QP band gaps of the other oxides SnO_2 , SnO , In_2O_3 , and SiO_2 . For that reason, Fig. 1 also contains the fundamental band gaps of rh - In_2O_3 (cf. Ref. 30), rt - SnO_2 (Ref. 31), lt - SnO (Refs. 32, 33), and β - SiO_2 (Refs. 34, 35) calculated within the HSE+ G_0W_0 approach. From this figure it can be seen that combining In_2O_3 , SnO_2 , and ZnO will allow for a tuning of the lattice constant, whereas the influence on the band gap remains small. Indeed, material combinations such as tin-doped indium oxide³⁶ or zinc-indium-tin oxide³⁷ exist. On the other hand, the introduction of SiO_2 should allow for a tuning of the band gap of the alloy without influencing the lattice parameter too much. Mixing ZnO with SnO can be a way to increase the lattice parameter in the alloy while, at the same time, decreasing the fundamental band gap even more than by alloying with CdO .

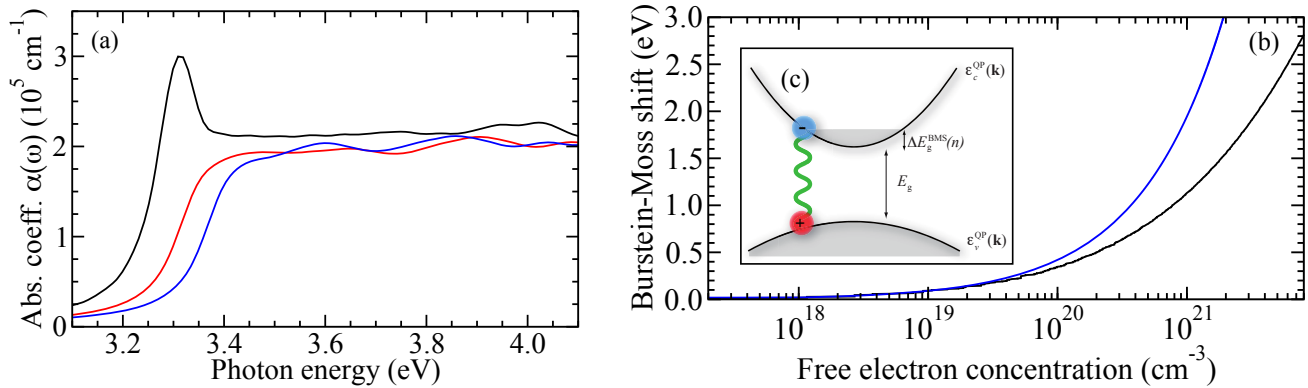


Figure 2. (Color online) (a) Calculated optical absorption coefficients of undoped (black) and n -doped ZnO for ordinary light polarization. A free-electron concentration of $n = 1.9 \times 10^{19} \text{ cm}^{-3}$ (red) or $n = 4.8 \times 10^{19} \text{ cm}^{-3}$ (blue) has been taken into account in the calculations. (b) Dependence of the Burstein-Moss shift (BMS) on the free-electron concentration as calculated from the full *ab-initio* approach (black curve) and the two-band model (red curve). (c) Visualization of the two-band model.

3. INFLUENCE OF n -DOPING

As pointed out before, the TCOs are typically n doped to significantly increase their conductivity, making them suitable for device applications. In ZnO samples, for instance, free-electron concentrations of more than $5 \times 10^{20} \text{ cm}^{-3}$ can be achieved by means of doping with aluminum¹⁴ or indium.¹⁵ The presence of such a degenerate electron gas in the CBs of any material is expected to strongly modify the optical properties, especially in the vicinity of the absorption onset. Therefore, we extended the Bethe-Salpeter approach to account for the partial occupation of the lowest CB states as well as for the impact on the screening of the electron-hole interaction.^{21,38}

As elucidated in Refs. 21, 38 the additional screening due to the free electrons in the lowest CB can be described within the Thomas-Fermi model for typical doping concentrations. In this case the presence of the free carriers modifies the screened electron-hole interaction in such a way that it can be described by a Yukawa potential with an inverse screening length that is calculated from the respective free-electron density. In addition, the degenerate electron gas occupies the lowest CB states which is why the respective optical transitions are forbidden [cf. schematic plot in Fig. 2(c)]. This Pauli blocking leads to an enlargement of the optical gap, which is also called BMS^{39,40} and whose magnitude depends on the density of the degenerate electron gas. By taking these effects into account when solving the BSE we are able to disentangle their interplay and we explain how they affect the optical-absorption properties.^{21,38} Ultimately, we investigate the combined effect of the modified electron-hole interaction and the Pauli blocking on the excitons.

Here we briefly summarize our results that we computed for the two free-electron concentrations of $1.9 \times 10^{19} \text{ cm}^{-3}$ and $4.8 \times 10^{19} \text{ cm}^{-3}$ in *wz*-ZnO.^{21,38} Figure 2(a) shows the optical absorption coefficient calculated for undoped ZnO as well as the results computed for these two cases with doping. From comparing these curves it is clear that already for moderately large free-electron densities the additional screening is strong and the characteristic excitonic peak at the absorption onset of undoped ZnO is not visible anymore. In addition, the effect of the BMS is visible as the absorption onset occurs at higher photon energies with increasing free-electron concentration. Comparison to experiment⁴¹ shows excellent agreement, as discussed in detail in Refs. 21, 38.

Since the Yukawa potential, as a short-range interaction, has no bound states for screening lengths below a certain value^{42,43} (i.e. for free-electron concentrations that exceed a critical value) the possibility of an excitonic Mott transition is discussed in the literature.⁴⁴ Mahan studied this question for a two-band system consisting of one filled valence band and additional free electrons in the lowest CB and concluded that the Pauli blocking modifies the electron-hole interaction in such a way that the bound excitonic state does not vanish for finite free-electron concentrations.⁴⁵ Instead, a Mahan exciton with modified binding energies and oscillator strengths persists. Using the results of our *ab-initio* calculations of the exciton binding energy (and oscillator strength) of the lowest bound electron-hole pair state we confirm Mahan's findings for ZnO.^{21,38} However, we find a rather continuous decrease of the binding energy and the oscillator strength such that it is difficult to exclude the Mott transition based on measured absorption spectra.

In order to quantify the Burstein-Moss shift we compare in Fig. 2(b) results obtained from the band structure that has been used to set up the excitonic Hamiltonian to numbers computed in a parabolic two-band model. Assuming a parabolic

valence and a parabolic CB [cf. Fig. 2(c)] and using the valence-band maximum as energy zero, the BMS $\Delta E_g^{\text{BMS}}(n_c)$ immediately follows from

$$\Delta E_g^{\text{BMS}}(n_c) = \epsilon_c^{\text{QP}}(k_c) - \epsilon_v^{\text{QP}}(k_c) - E_g = \frac{\hbar^2 k_c^2}{2m_c} + \frac{\hbar^2 k_c^2}{2m_v}, \quad (1)$$

where m_c and m_v are the effective masses of the CB and the valence band, respectively, and n_c denotes the free-electron concentration in the material. This free-electron concentration is related to the respective Fermi vector k_c by means of

$$k_c = (3\pi^2 n_c)^{\frac{1}{3}}. \quad (2)$$

Using Eq. (2) and the definition of the reduced mass of the electron-hole pair, $\mu = m_c m_v / (m_c + m_v)$, Eq. (1) becomes

$$\Delta E_g^{\text{BMS}}(n_c) = \frac{\hbar^2 k_c^2}{2\mu} = \frac{\hbar^2 (3\pi^2 n_c)^{\frac{2}{3}}}{2\mu}. \quad (3)$$

For ZnO we use $m_c = 0.3 m$ and $m_v = 0.5 m$ (cf. Ref. 46) to evaluate Eq. (3), m being the free-electron mass, and compare the result to our findings from the full band structure in Fig. 2(b). This figure clearly points out how the approximate treatment within the two-band model is only valid for small free-carrier concentrations. Already for experimentally easily achievable concentrations of about $2 \times 10^{20} \text{ cm}^{-3}$ the difference is larger than 0.1 eV due to the non-parabolicity of the corresponding bands. Only when the occupation of the CB is restricted to the close vicinity of the Γ point, the parabolic model is a good approximation.

We also want to emphasize that in addition to the BMS there is the so-called band-gap renormalization due to the free carriers in the system. In Refs. 21, 38 this many-body effect is described using the model given by Berggren and Sernelius,^{47,48} which leads to an effective band-gap shrinkage almost as large as the band-gap increase due to the BMS.^{21,38}

4. SUMMARY

In this paper we outlined how the HSE+ G_0W_0 approach in combination with a cluster-expansion scheme can be applied to study, for instance, the fundamental band gap of $\text{Mg}_x\text{Zn}_{1-x}\text{O}$ and $\text{Cd}_x\text{Zn}_{1-x}\text{O}$ alloys. From the comparison of the configurational averages to the fundamental band gaps of other TCOs we pointed out what the respective effect on the band gaps or the lattice parameters are, when these materials are combined for device applications.

In addition, we summarized our extension of the BSE first-principles approach to consistently account for the band-gap renormalization, the Pauli blocking of optical transitions, the reduction of the electron-hole attraction, and the occupation-induced modifications of the electron-hole interaction that occur in n -doped materials. This parameter-free framework has previously been shown to describe the frequency-dependent absorption coefficient of n -ZnO, especially around the onset, in excellent agreement with experimental results and is capable of describing the Mahan-like exciton in the doped system. The dependence of the Burstein-Moss shift on the free-carrier concentration has been discussed.

Acknowledgments

We thank Jérôme Steinhauser for fruitful discussions. The research presented here has received funding from the European Community's Seventh Framework Programme (FP7/2007-2013) under grant agreement No. 211956 and from the Deutsche Forschungsgemeinschaft (Project No. Be1346/20-1). Part of this work was performed under the auspices of the U.S. Department of Energy at Lawrence Livermore National Laboratory under Contract DE-AC52-07A27344.

REFERENCES

- [1] Ginley, D. S. and Bright, C., "Transparent conducting oxides," *MRS Bull.* **25**, 15–18 (2000).
- [2] Ramirez, A. P., "Oxide electronics emerge," *Science* **315**(5817), 1377–1378 (2007).
- [3] Fortunato, E., Ginley, D., Hosono, H., and Paine, D. C., "Transparent conducting oxides for photovoltaics," *MRS Bull.* **32**, 242–247 (2007).
- [4] Lunt, R. R. and Bulovic, V., "Transparent, near-infrared organic photovoltaic solar cells for window and energy-scavenging applications," *Appl. Phys. Lett.* **98**(11), 113305 (2011).

- [5] Schleife, A., Fuchs, F., Furthmüller, J., and Bechstedt, F., “First-principles study of ground- and excited-state properties of MgO, ZnO, and CdO polymorphs,” *Phys. Rev. B* **73**(24), 245212 (2006).
- [6] Schleife, A., Rödl, C., Fuchs, F., Furthmüller, J., Bechstedt, F., Jefferson, P. H., Veal, T. D., McConville, C. F., Piper, L. F. J., DeMasi, A., Smith, K. E., Lösch, H., Goldhahn, R., Cobet, C., Zúñiga-Pérez, J., and Muñoz-Sanjosé, V., “*Ab-initio* studies of electronic and spectroscopic properties of MgO, ZnO, and CdO,” *J. Korean Phys. Soc.* **53**(5), 2811–2815 (2008).
- [7] Schleife, A., Rödl, C., Fuchs, F., Furthmüller, J., and Bechstedt, F., “Optical and energy-loss spectra of MgO, ZnO, and CdO from ab initio many-body calculations,” *Phys. Rev. B* **80**(3), 035112 (2009).
- [8] King, P. D. C., Veal, T. D., Schleife, A., Zúñiga-Pérez, J., Martel, B., Jefferson, P. H., Fuchs, F., Muñoz-Sanjosé, V., Bechstedt, F., and McConville, C. F., “Valence-band electronic structure of CdO, ZnO, and MgO from x-ray photoemission spectroscopy and quasi-particle-corrected density-functional theory calculations,” *Phys. Rev. B* **79**(20), 205205 (2009).
- [9] Piper, L. F. J., DeMasi, A., Smith, K. E., Schleife, A., Fuchs, F., Bechstedt, F., Zúñiga-Pérez, J., and Muñoz-Sanjosé, V., “Electronic structure of single-crystal rocksalt CdO studied by soft x-ray spectroscopies and ab initio calculations,” *Phys. Rev. B* **77**(12), 125204 (2008).
- [10] Preston, A. R. H., Ruck, B. J., Piper, L. F. J., DeMasi, A., Smith, K. E., Schleife, A., Fuchs, F., Bechstedt, F., Chai, J., and Durbin, S. M., “Band structure of ZnO from resonant x-ray emission spectroscopy,” *Phys. Rev. B* **78**(15), 155114 (2008).
- [11] Ohtomo, A. and Tsukazaki, A., “Pulsed laser deposition of thin films and superlattices based on ZnO,” *Semicond. Sci. Tech.* **20**(4), S1–S12 (2005).
- [12] Schmidt, R., Rheinländer, B., Schubert, M., Spemann, D., Butz, T., Lenzner, J., Kaidashev, E. M., Lorenz, M., Rahm, A., Semmelhack, H. C., and Grundmann, M., “Dielectric functions (1 to 5 eV) of wurtzite $\text{Mg}_x\text{Zn}_{1-x}\text{O}$ (≤ 0.29) thin films,” *Appl. Phys. Lett.* **82**(14), 2260–2262 (2003).
- [13] Sadofev, S., Blumstengel, S., Cui, J., Puls, J., Rogaschewski, S., Schäfer, P., Sadofyev, Y. G., and Henneberger, F., “Growth of high-quality ZnMgO epilayers and ZnO/ZnMgO quantum well structures by radical-source molecular-beam epitaxy on sapphire,” *Appl. Phys. Lett.* **87**(9), 091903 (2005).
- [14] Sernelius, B. E., Berggren, K.-F., Jin, Z.-C., Hamberg, I., and Granqvist, C. G., “Band-gap tailoring of ZnO by means of heavy Al doping,” *Phys. Rev. B* **37**(17), 10244–10248 (1988).
- [15] Major, S., Banerjee, A., and Chopra, K., “Highly transparent and conducting indium-doped zinc oxide films by spray pyrolysis,” *Thin Solid Films* **108**(3), 333–340 (1983).
- [16] Schleife, A., Rödl, C., Furthmüller, J., and Bechstedt, F., “Electronic and optical properties of $\text{Mg}_x\text{Zn}_{1-x}\text{O}$ and $\text{Cd}_x\text{Zn}_{1-x}\text{O}$ from ab initio calculations,” *New J. Phys.* **13**(8), 085012 (2011).
- [17] Sadofev, S., Blumstengel, S., Cui, J., Puls, J., Rogaschewski, S., Schäfer, P., and Henneberger, F., “Visible band-gap ZnCdO heterostructures grown by molecular beam epitaxy,” *Appl. Phys. Lett.* **89**(20), 201907 (2006).
- [18] Lai, H. H.-C., Kuznetsov, V. L., Egdell, R. G., and Edwards, P. P., “Electronic structure of ternary $\text{Cd}_x\text{Zn}_{1-x}\text{O}$ ($0 \leq x \leq 0.075$) alloys,” *Appl. Phys. Lett.* **100**(7), 072106 (2012).
- [19] Schleife, A., Eisenacher, M., Rödl, C., Fuchs, F., Furthmüller, J., and Bechstedt, F., “Ab initio description of heterostructural alloys: Thermodynamic and structural properties of $\text{Mg}_x\text{Zn}_{1-x}\text{O}$ and $\text{Cd}_x\text{Zn}_{1-x}\text{O}$,” *Phys. Rev. B* **81**(24), 245210 (2010).
- [20] Schleife, A., *Exciting Imperfection: Real-structure effects in magnesium-, cadmium-, and zinc-oxide*, PhD thesis, Friedrich-Schiller-Universität, Jena (2010).
- [21] Schleife, A., [*Electronic and optical properties of MgO, ZnO, and CdO*], Südwestdeutscher Verlag für Hochschulschriften (2011).
- [22] Heyd, J., Scuseria, G. E., and Ernzerhof, M., “Erratum: “Hybrid functionals based on a screened coulomb potential” [J. Chem. Phys. **118**, 8207 (2003)],” *J. Chem. Phys.* **124**(21), 219906 (2006).
- [23] Paier, J., Marsman, M., Hummer, K., Kresse, G., Gerber, I. C., and Ángyán, J. G., “Screened hybrid density functionals applied to solids,” *J. Chem. Phys.* **124**(15), 154709 (2006).
- [24] Paier, J., Marsman, M., Hummer, K., Kresse, G., Gerber, I. C., and Ángyán, J. G., “Erratum: “Screened hybrid density functionals applied to solids” [J. Chem. Phys. **124**, 154709 (2006)],” *J. Chem. Phys.* **125**(24), 249901 (2006).
- [25] Strinati, G., “Application of the Green’s functions method to the study of the optical properties of semiconductors,” *Riv. Nuovo Cimento* **11**(12), 1–86 (1988).

- [26] Onida, G., Reining, L., and Rubio, A., “Electronic excitations: density-functional versus many-body Green’s-function approaches,” *Rev. Mod. Phys.* **74**(2), 601–659 (2002).
- [27] Chen, A.-B. and Sher, A., [*Semiconductor Alloys*], Plenum, New York (1995).
- [28] Teles, L. K., Furthmüller, J., Scolaro, L. M. R., Leite, J. R., and Bechstedt, F., “First-principles calculations of the thermodynamic and structural properties of strained $\text{In}_x\text{Ga}_{1-x}\text{N}$ and $\text{Al}_x\text{Ga}_{1-x}\text{N}$ alloys,” *Phys. Rev. B* **62**(4), 2475–2485 (2000).
- [29] Sher, A., van Schilfgaarde, M., Chen, A.-B., and Chen, W., “Quasichemical approximation in binary alloys,” *Phys. Rev. B* **36**(8), 4279–4295 (1987).
- [30] Fuchs, F. and Bechstedt, F., “Indium-oxide polymorphs from first principles: Quasiparticle electronic states,” *Phys. Rev. B* **77**(15), 155107 (2008).
- [31] Schleife, A., Varley, J. B., Fuchs, F., Rödl, C., Bechstedt, F., Rinke, P., Janotti, A., and Van de Walle, C. G., “Tin dioxide from first principles: Quasiparticle electronic states and optical properties,” *Phys. Rev. B* **83**(3), 035116 (2011).
- [32] Küfner, S., *Ab-initio Untersuchung von Zinnmonoxid- und Zindioxidoberflächen*, Master’s thesis, Friedrich-Schiller-University Jena (2011).
- [33] Küfner, S., Schleife, A., and Bechstedt, F. unpublished (2012).
- [34] Fuchs, F. (2011). Private communication.
- [35] Höffling, B., Schleife, A., Rödl, C., and Bechstedt, F., “Band discontinuities at Si-TCO interfaces from quasiparticle calculations: Comparison of two alignment approaches,” *Phys. Rev. B* **85**, 035305 (2012).
- [36] Tahar, R. B. H., Ban, T., Ohya, Y., and Takahashi, Y., “Tin doped indium oxide thin films: Electrical properties,” *J. Appl. Phys.* **83**(5), 2631–2645 (1998).
- [37] Buchholz, D. B., Liu, J., Marks, T. J., Zhang, M., and Chang, R. P. H., “Control and characterization of the structural, electrical, and optical properties of amorphous Zinc-Indium-Tin oxide thin films,” *ACS Applied Materials & Interfaces* **1**(10), 2147–2153 (2009).
- [38] Schleife, A., Rödl, C., Fuchs, F., Hannewald, K., and Bechstedt, F., “Optical absorption in degenerately doped semiconductors: Mott transition or Mahan excitons?,” *Phys. Rev. Lett.* **107**, 236405 (2011).
- [39] Burstein, E., “Anomalous optical absorption limit in InSb,” *Phys. Rev.* **93**(3), 632–633 (1954).
- [40] Moss, T. S., “The interpretation of the properties of indium antimonide,” *Proc. Phys. Soc. B* **67**(10), 775 (1954).
- [41] Makino, T., Tamura, K., Chia, C. H., Segawa, Y., Kawasaki, M., Ohtomo, A., and Koinuma, H., “Optical properties of ZnO:Al epilayers: Observation of room-temperature many-body absorption-edge singularity,” *Phys. Rev. B* **65**(12), 121201 (2002).
- [42] Glutsch, S., [*Excitons in Low-Dimensional Semiconductors: Theory, Numerical Methods, Applications*], Springer (2004).
- [43] Li, Y., Luo, X., and Kröger, H., “Bound states and critical behavior of the Yukawa potential,” *Sci. China Ser. G* **49**(1), 60–71 (2006).
- [44] Klingshirn, C., Hauschild, R., Fallert, J., and Kalt, H., “Room-temperature stimulated emission of ZnO: Alternatives to excitonic lasing,” *Phys. Rev. B* **75**(11), 115203 (2007).
- [45] Mahan, G. D., “Excitons in degenerate semiconductors,” *Phys. Rev.* **153**(3), 882–889 (1967).
- [46] Schleife, A., Fuchs, F., Rödl, C., Furthmüller, J., and Bechstedt, F., “Band-structure and optical-transition parameters of wurtzite MgO, ZnO, and CdO from quasiparticle calculations,” *Phys. Status Solidi B* **246**(9), 2150–2153 (2009).
- [47] Berggren, K. F. and Sernelius, B. E., “Band-gap narrowing in heavily doped many-valley semiconductors,” *Phys. Rev. B* **24**(4), 1971–1986 (1981).
- [48] Wu, J., Walukiewicz, W., Shan, W., Yu, K. M., Ager, J. W., Haller, E. E., Lu, H., and Schaff, W. J., “Effects of the narrow band gap on the properties of InN,” *Phys. Rev. B* **66**(20), 201403 (2002).